**Indonesian Journal of Electrical Engineering and Computer Science**
Vol. 30, No. 1, April 2023, pp. 510~517
ISSN: 2502-4752, DOI: 10.11591/ijeecs.v30.i1.pp510-517


# Discriminative analysis of wavelets for efficient medical image compression

**Deepa Sivaraman, Jeneetha Jebanazer, Bhuvaneswari Balasubramanian**
Department of Electronics and Communication Engineering, Panimalar Engineering College, Chennai, India

**Article Info**

***Article history:***

Received Jul 4, 2022
Revised Dec 11, 2022
Accepted Dec 20, 2022

***Keywords:***

Compression ratio
Daubechies
Haar
Image compression
Mean square error

**ABSTRACT**

Critical diagnostic information inferred using state of the artradiology techniques helps radiologists in determining the severity of diseases and hence suggest suitable treatment procedures. As a result, dealing with medical image compression necessitates a trade-off between good perceptual quality and high compression rate. The objective of this work is twofold, i) to investigate the effect of increasing the number of encoding loops on medical image compression parameters, and ii) to determine the most suitable wavelet for medical image compression. Haar, Daubechies, Biorthogonal Demeyer, Coifletand Symlet wavelets are used for comparison. Six different sets of medical images are used for testing and from the results obtained it is observed that increasing the number of encoding loops results in better compression parameters but increasing beyond 9 has no significant effect on compression parameters and thus the optimum choice for the number of encoding loops is 9. From the second analysis it is observed that changing the type of wavelets used has no significant effect on the compression parameters.

*This is an open access article under the CC BY-SA license.*

***Corresponding Author:***

Deepa Sivaraman
Department of Electronics and Communication Engineering, Panimalar Engineering College
Chennai, India
Email: dineshdeepas1977@gmail.com

## 1. INTRODUCTION

Hospitals and health care centers generate huge number of medical images such as Magnetic resonance elastography (MRE), magnet resonance imaging (MRI), computed axial tomography (CAT), and ultra sound (US). which are loaded with critical radiological information. Secure storage and digital transmission of medical images, reports, and other therapeutically pertinent data is handled by a variety of systems, such as radiology information system (RIS) and patient archival and communication systems (PACS). Handling large volume of images is a challenging task for these data handling systems, thus demanding the need for high bit rate compression techniques. Lossy image compression techniques, though efficient in achieving good compression, may result in false diagnosis due to information loss. Thus, lossless compression techniques are most frequently used to compress medical images [1]-[3], so that the decompressed image is lossless in terms of aesthetics and diagnostics. Image compression techniques falls into various categories such as transform-based, machine learning-based, fractal-based, contextual-based and other hybrid methods. Though, transform-based compression techniques are computationally complex, the compression rate achieved is higher compared to other methods. Of the available popularly used transforms such as discrete cosine transform (DCT), ripplet transform, discrete wavelet transforms (DWT), radon transform, and contourlet transform wavelet transform is the most powerful one which can produce compressed images at higher compression ratios with higher peak to signal noise ratio (PSNR) values [4].

Wavelet exhibits exceptional de-correlation property and supports multi-resolution analysis (MRA) making it the most preferable image transformation technique and is predominantly used in several standards such as JPEG2000 and MPEG-2/4. The transform coefficients are to be encoded at the transmitter end to achieve compression and decoded at the receiver end to decompress. Codec algorithms are used to compress the transform coefficients and play the most significant role in achieving higher compression rate. Embedded zerotree wavelet (EZW), spatial-orientation tree wavelet (STW) [5]-[7], set partitioning in hierarchical trees (SPIHT), 3D-Set partitioning in hierarchical trees (3D-SPIHT) [8]-[12], Adaptively scanned wavelet difference reduction (ASWDR) algorithm proposed by Walker [13] and wavelet difference reduction (WDR) algorithm [14]-[16] are the most popularly used codec algorithms. Feature preserving image compression techniques and contextual based image compression techniques are also found to be promising techniques to compress medical images [17]-[24]. Manigandan and Deepa [25], carried out a comprehensive analysis to determine the most efficient encoding technique, and from the results obtained, it is evident that EZW and STW algorithms prove to minimize the mean square error. Minimum MSE of images, guarantees fault free diagnosis. Thus, in this paper, EZW algorithm is used to compress the transform coefficient and investigations are carried out to understand the effect of increasing the number of encoding loops on the compression parameters. In the second analysis, the performance of various wavelets is compared to determine the most efficient wavelet for medical image compression.

## 2. METHODS

In DWT, analysis filter bank and synthesis filter bank are employed in the transmitter end and receiver end, respectively. Appropriate wavelet (such as Haar, Symlet, or Coiflet) and number of levels (n) for the decomposition are selected in the first stage. The approximation, vertical detail, horizontal detail, and diagonal detail subbands are created from the input images by the analysis filter bank. The detail coefficients are thresholded from scales J-1 to J-n in the second stage. An example of wavelet decomposition is shown in Figure 1. Figure 1(a) shows the original MRI image, Figure 1(b) shows the wavelet decomposed image, and Figure 1(c) shows decompressed image.

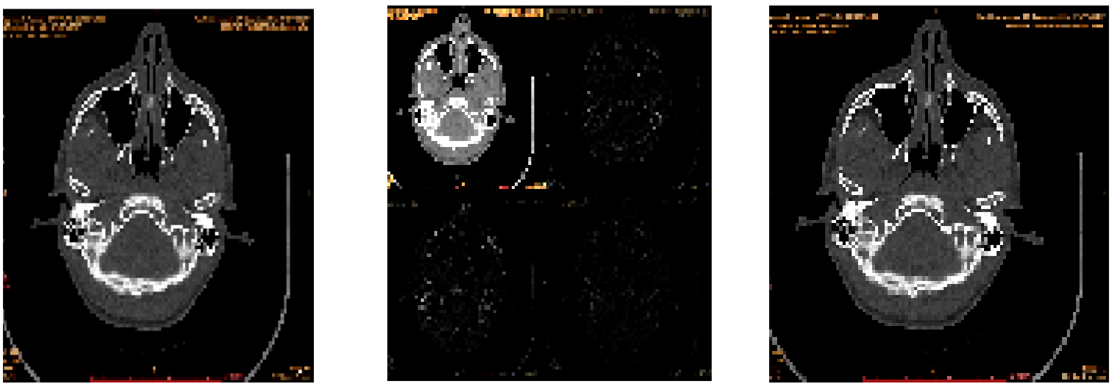

(a) (b) (c)

Figure 1. Compression of MRI image using wavelet decomposition: (a) original MRI image, (b) first level decomposition, and (c) decompressed image

### 2.1. Performance measures

The decompressed image might not be the same as the original image when the compression is lossy in nature. A high compression ratio results in the loss of more visual features. Finding the ideal balance between a high compression ratio and a decent perceptual result is the problem presented by compression techniques. The compression ratio (CR), mean square error (MSE), peak signal to noise ratio (PSNR), maximum error, L2-Norm Ratio, and bits per pixel are the metrics used to compare the different image compression approaches (BPP).

### 2.2. Proposed analysis 1

In the first analysis, the effect of changing the number of encoding loops on the performance measures is analyzed. In this analysis, the wavelet and the encoding method are fixed, whereas the number of encoding loops is varied and its effect on compression parameters is analyzed. Initially, the input image is decomposed using Haar wavelet transform and the transformed coefficients are encoded using EZW coding. The number of encoding loops can vary from 1 to 9. The input image is compressed, and the compression parameters are computed by varying the number of encoding loops from 1 to 9. The flow diagram is shown in Figure 2.

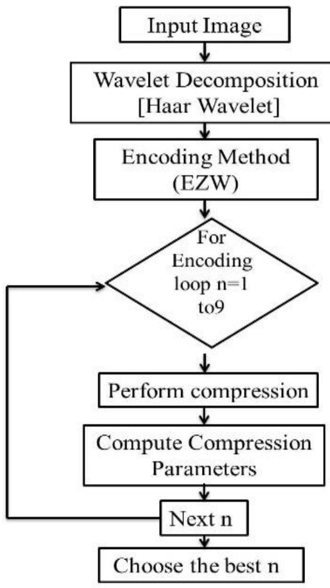


Figure 2. Flowchart of proposed analysis 1

Various performance metrics are obtained and the graphs are plotted as shown in Figure 3. MSE obtained for various input images are tabulated in Table 1 and Figure 3(a) shows the graph of the same. From the graph, it is clear, that as the number of encoding loops is increased the MSE decreases, thus improving the quality of the decompressed image. Increasing the encoding loops beyond 9 does not have any significant effect on MSE.

Table 2 shows the maximum error obtained for various input images and Figure 3(b) shows the graph of the same. From the graph it is clear, that as the number of encoding loops is increased the ME decreases, thus improving the quality of the decompressed image. Increasing the encoding loops beyond 9 does not have any significant effect on ME. Table 3 shows the L2 normal ratio obtained for various input images and Figure 3(c) shows the graph of the same. From the graph, it is clear that as the number of encoding loops is increased the L2 normal ratio increases, thus improving the quality of the decompressed image. Increasing the encoding loops beyond 9 does not have any significant effect on L2 normal ratio. Table 4 shows the peak signal noise to ratio (PSNR) obtained for various input images and Figure 3(d) shows the graph of the same. From the graph, it is clear that as the number of encoding loops is increased the PSNR increases, thus improving the quality of the decompressed image. Increasing the encoding loops beyond 9 does not have any significant effect on PSNR.

Table 5 shows the Bits Per Pixel obtained for various input images and Figure 3(e) shows the graph of the same. From the graph, it is clear that as the number of encoding loops is increased the B.P.P increases, thus improving the quality of the decompressed image. Increasing the encoding loops beyond 9 does not have any significant effect on B.P.P. Table 6 shows the compression ratio obtained for various input images and Figure 3(f) shows the graph of the same. From the graph, it is clear that as the number of encoding loops is increased the CR increases, thus improving the quality of the decompressed image. Increasing the encoding loops beyond 9 does not have any significant effect on CR.

Table 1. Mean square error obtained using Haar wavelet and EZW encoding method

| Image Type | No. of Encoding Loops | | | | | | | | |
|---|---|---|---|---|---|---|---|---|---|
| | 1 | 2 | 3 | 4 | 5 | 6 | 7 | 8 | 9 |
| Ultrasound | 3559 | 342.6 | 55.45 | 20.81 | 10.75 | 4.717 | 1.363 | 0.363 | 0.05601 |
| XRAY | 1661 | 1724 | 43.68 | 23.63 | 6.79 | 3.357 | 1.411 | 0.3904 | 0.3904 |
| CT Scan | 1878 | 739.1 | 231.2 | 72.48 | 24.77 | 7.005 | 1.692 | 0.2941 | 0.04453 |
| MRI 1 | 1476 | 853.5 | 105.6 | 28.79 | 8.219 | 2.426 | 0.5577 | 0.09416 | 0.0148 |
| / | 2680 | 282.1 | 103.7 | 31.7 | 9.382 | 3.179 | 0.08084 | 0.134 | 0.02082 |

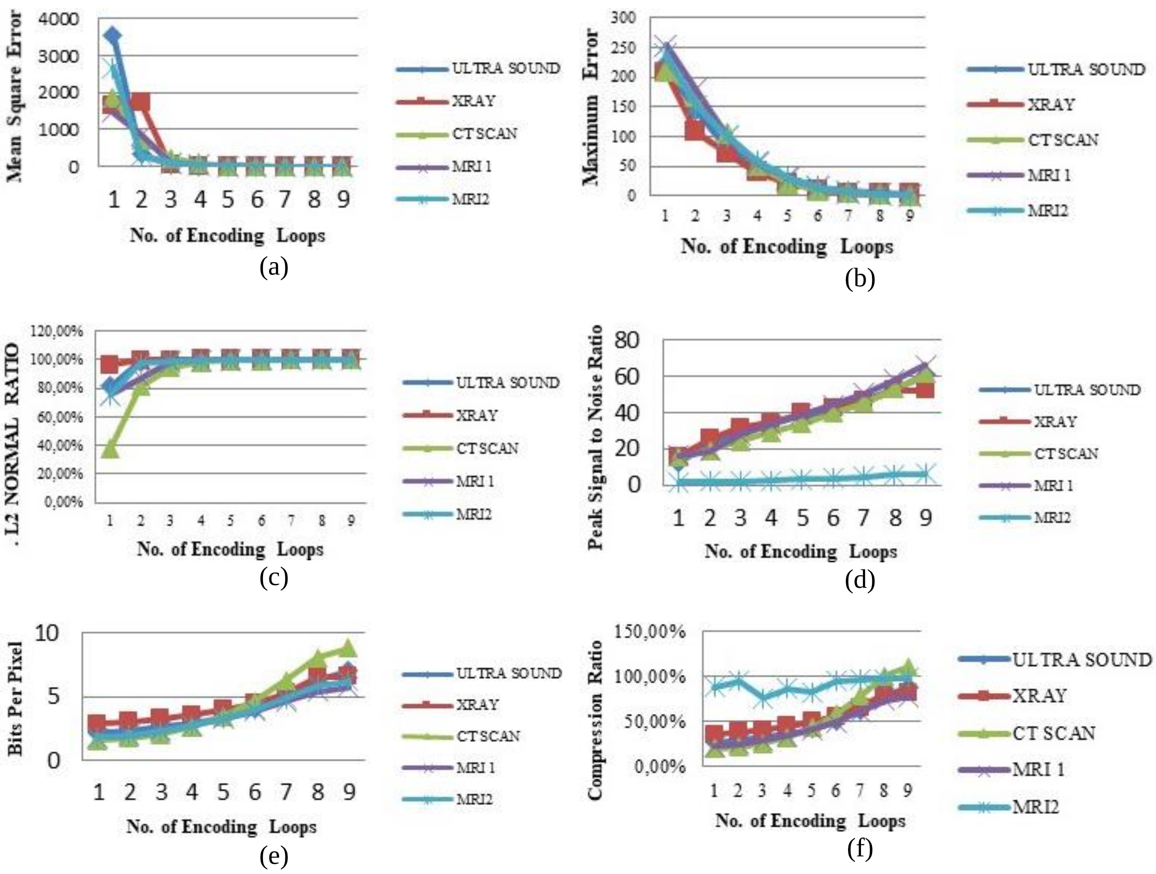


Figure 3. Performance measures: (a) MSE, (b) Max error, (c) L2 normal ratio, (d) PSNR, (e) BPP, and (f) CR obtained using Haar wavelet and EZW encoding method by varying the number of encoding loops

Table 2. Maximum error obtained using Haar wavelet and EZW encoding method

| Image Type | No. of Encoding Loops | | | | | | | | |
|---|---|---|---|---|---|---|---|---|---|
| | 1 | 2 | 3 | 4 | 5 | 6 | 7 | 8 | 9 |
| Ultrasound | 218 | 145 | 81 | 50 | 23 | 13 | 6 | 3 | 2 |
| XRAY | 208 | 108 | 73 | 40 | 22 | 10 | 5 | 3 | 3 |
| CT Scan | 209 | 168 | 105 | 53 | 22 | 11 | 7 | 3 | 1 |
| MRI 1 | 253 | 179 | 100 | 55 | 30 | 15 | 7 | 4 | 2 |
| MRI2 | 238 | 152 | 101 | 59 | 31 | 15 | 7 | 3 | 2 |

Table 3. L2 normal ratio obtained using Haar wavelet and EZW encoding method

| Image Type | No. of Encoding Loops | | | | | | | | |
|---|---|---|---|---|---|---|---|---|---|
| | 1 | 2 | 3 | 4 | 5 | 6 | 7 | 8 | 9 |
| Ultrasound | 81.51% | 98.37% | 99.74% | 99.91% | 99.95% | 99.98% | 99.99% | 100.00% | 100.00% |
| X-RAY | 96.52% | 99.64% | 99.91% | 99.95% | 99.99% | 99.99% | 100.00% | 100.00% | 100.00% |
| CT Scan | 38.18% | 81.47% | 94.59% | 98.34% | 99.44% | 99.84% | 99.96% | 99.99% | 100.00% |
| MRI 1 | 75.81% | 86.84% | 98.47% | 99.58% | 99.88% | 99.97% | 99.99% | 100.00% | 100.00% |
| MRI2 | 75.63% | 97.72% | 99.17% | 99.75% | 99.93% | 99.97% | 99.99% | 100.00% | 100.00% |

Table 4. Peak signal to noise ratio obtained using Haar wavelet and EZW encoding method

| Image Type | No. of Encoding Loops | | | | | | | | |
|---|---|---|---|---|---|---|---|---|---|
| | 1 | 2 | 3 | 4 | 5 | 6 | 7 | 8 | 9 |
| Ultrasound | 12.62 | 22.78 | 30.7 | 35.09 | 37.82 | 41.39 | 46.79 | 53.22 | 60.65 |
| XRAY | 15.93 | 25.77 | 31.7 | 34.4 | 39.81 | 42.87 | 46.64 | 52.22 | 52.22 |
| CT Scan | 15.39 | 19.44 | 24.5 | 29.53 | 34.19 | 39.68 | 45.85 | 53.45 | 61.64 |
| MRI 1 | 16.44 | 18.82 | 27.9 | 33.54 | 38.98 | 44.28 | 50.67 | 58.39 | 66.43 |
| MRI2 | 1.7999 | 1.9937 | 2.29 | 2.7281 | 3.2917 | 3.9642 | 4.8627 | 5.8522 | 6.2035 |

Table 5. Bits per pixel obtained using Haar wavelet and EZW encoding method

| Image Type | No. of Encoding Loops | | | | | | | | |
|---|---|---|---|---|---|---|---|---|---|
| | 1 | 2 | 3 | 4 | 5 | 6 | 7 | 8 | 9 |
| Ultrasound | 2.1475 | 2.3527 | 2.6201 | 2.9434 | 3.3519 | 3.9976 | 5.026 | 6.334 | 7.0597 |
| XRAY | 2.8784 | 3.0659 | 3.3027 | 3.5994 | 3.9851 | 4.4869 | 5.27 | 6.564 | 6.5643 |
| CT Scan | 1.5758 | 1.7312 | 2.0745 | 2.6339 | 3.4557 | 4.6649 | 6.267 | 8.081 | 8.8457 |
| MRI 1 | 1.8007 | 1.9771 | 2.3174 | 2.7378 | 3.2683 | 3.8883 | 4.635 | 5.426 | 5.7591 |
| MRI2 | 1.7991 | 1.9937 | 2.2898 | 2.7281 | 3.2917 | 3.9642 | 4.863 | 5.852 | 6.2235 |

Table 6. Compression ratio obtained using Haar wavelet and EZW encoding method

| Image Type | No. of Encoding Loops | | | | | | | | |
|---|---|---|---|---|---|---|---|---|---|
| | 1 | 2 | 3 | 4 | 5 | 6 | 7 | 8 | 9 |
| Ultrasound | 26.84% | 29.41% | 32.75% | 36.75% | 41.90% | 49.90% | 62.83% | 79.17% | 88.25% |
| XRAY | 35.98% | 38.32% | 41.28% | 44.99% | 49.81% | 56.09% | 65.87% | 81.30% | 81.30% |
| CT Scan | 19.70% | 21.64% | 25.93% | 32.93% | 43.20% | 58.31% | 78.34% | 101.01% | 110.57% |
| MRI 1 | 22.51% | 24.71% | 28.97% | 34.22% | 41.15% | 49.55% | 60.78% | 73.15% | 77.79% |
| MRI2 | 88.25% | 95.37% | 75.94% | 86.33% | 82.78% | 95.37% | 98.46% | 97.80% | 101.41% |

### 2.3. Proposed analysis 2

In the second analysis, the effect of changing the type of wavelet on the performance measures is analyzed. From analysis 1, it is clear that the best result is produced for number of encoding loops equal to 9, thus for this analysis the number of encoding loops is fixed as 9 and the type of compression algorithm is fixed as 3-D SPIHT, the wavelet filters are varied, and the compression parameters are computed. The proposed flowchart is shown in Figure 4. The various wavelets used for analysis are Haar, Daubechies, Coiflets, Symlet, Biorthogonal, Reverse Biorthogonal, Discrete FIR Meyer wavelet and Fejer-Korovkin wavelets.

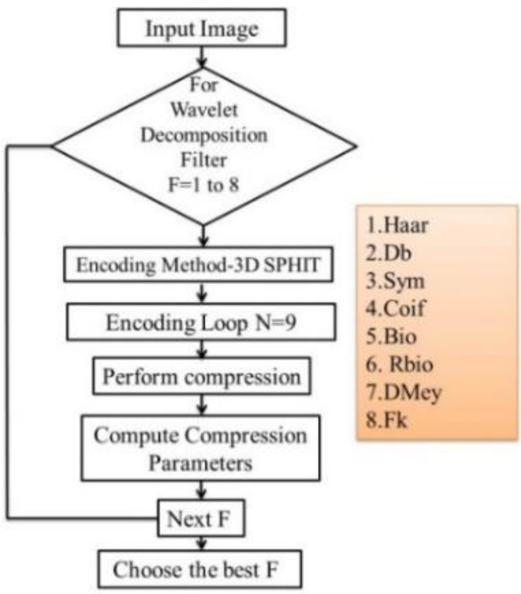


Figure 4. Flowchart of proposed analysis 2

For each type of wavelet, the level of decomposition is set as one, and 3-D SPIHT compression algorithm with 9 encoding loops are used for analysis. Figure 5 shows the various performance metrics obtained. Figures 5(a) and (b) show the mean square error and the maximum error obtained respectively for various types of wavelets. The other compression parameters L2 normal ratio, PSNR, BPP and CR obtained by varying the type of wavelets are shown in Figures 5(c)-(f) respectively. From the graphs, it is evident that the type of wavelet does not have a great impact on the compression parameters obtained. Figure 6 shows the output images obtained using Haar wavelets on different types of medical images. Figure 6(a) shows the input images, Figure 6(b) shows the wavelet decomposed images, and Figure 6(c) shows the decompressed images obtained using Haar wavelets.

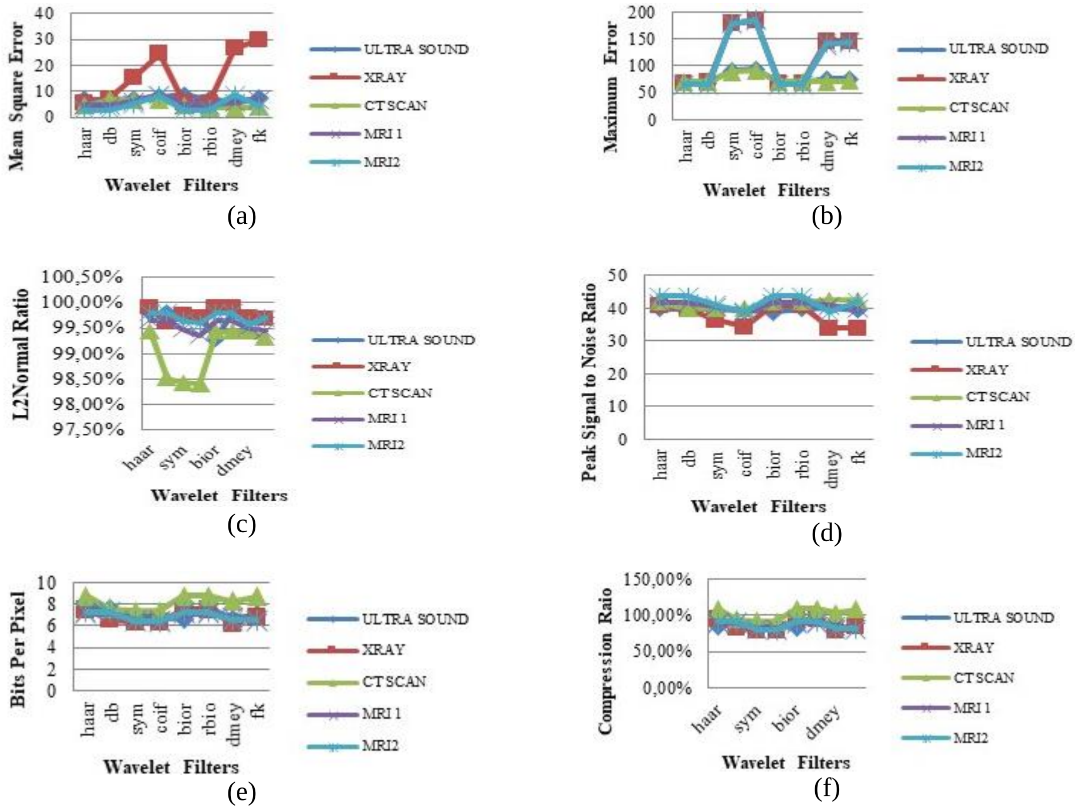


Figure 5. Performance measures: (a) MSE, (b) max error, (c) L2 normal ratio, (d) PSNR, (e) BPP, and (f) CR obtained for various wavelet filter functions

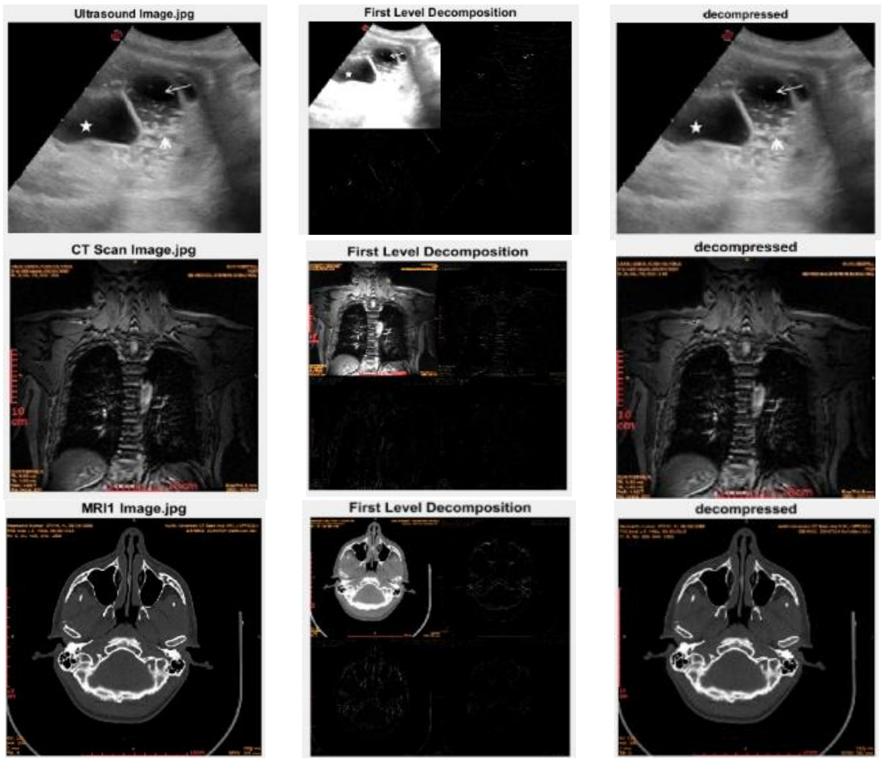


(a) (b) (c)

Figure 6. Output obtained on various images: (a) input image, (b) wavelet decomposed image, and (c) decompressed image obtained using Haar wavelets

## 3. RESULTS AND DISCUSSIONS

The results obtained using the proposed methods cannot be compared directly with the reported work in literature since the input images used by researchers are not the same and the size of the images also vary. Thus, the obtained results are compared with other significant methods found in literature. Four different and significant transform-based methods are considered for comparison, i) discrete cosine transform with SPIHT encoding, ii) contourlet transform with SPIHT encoding, iii) ripplet transform, and iv) curvelet transform based image compression techniques are used for comparison. For five test images, all the experiments are conducted using MATLAB 2014a for both the existing techniques reported in literature and the methods proposed in this paper. The performance metrics obtained are tabulated in Table 7. The proposed method 1, with Haar wavelets and 9 encoding loops has performed better in terms of performance measures and from the tabulated values, it is observed that modifying the type of wavelet has no significance on image compression.

Table 7. Comparison of the proposed methods with other existing techniques

| Image type | DCT-SPIHT | Contourlet-SPIHT | Ripplet | Curvelet | Proposed method1 | Proposed analysis 2 |
|---|---|---|---|---|---|---|
| | | | Mean square error | | | |
| Ultra sound | 1.0123 | 0.0986 | 0.0864 | 0.0923 | 0.05601 | 0.07275 |
| XRAY | 1.428 | 1.326 | 1.346 | 1.196 | 0.3904 | 0.44 |
| CT scan | 0.0976 | 0.7426 | 0.0882 | 0.0812 | 0.04453 | 0.0547 |
| MRI 1 | 0.04356 | 0.396 | 0.0412 | 0.0402 | 0.0148 | 0.0139 |
| MRI2 | 0.0656 | 0.0586 | 0.0426 | 0.0428 | 0.02082 | 0.0215 |
| | | | PSNR | | | |
| Ultra sound | 34.56 | 40.12 | 41.22 | 45.62 | 60.65 | 39.51 |
| XRAY | 32.86 | 39.64 | 38.42 | 41.68 | 52.22 | 36.23 |
| CT scan | 39.88 | 39.06 | 39.78 | 45.82 | 61.64 | 39.97 |
| MRI 1 | 39.62 | 40.04 | 40.12 | 46.12 | 66.43 | 40.32 |
| MRI2 | 39.41 | 40.96 | 42.22 | 45.34 | 62.035 | 41.01 |
| | | | Compression Ratio | | | |
| Ultra sound | 81.26 | 83.52 | 82.28 | 86.89 | 88.25 | 85.75 |
| XRAY | 75.48 | 76.25 | 74.12 | 82.24 | 81.30 | 79.40 |
| CT scan | 88.41 | 100.06 | 88.46 | 91.26 | 110.57 | 92.15 |
| MRI 1 | 76.84 | 74.42 | 74.896 | 80.098 | 77.79 | 81.30 |
| MRI2 | 75.42 | 75.48 | 76.42 | 80.16 | 101.41 | 80.65 |

## 4. CONCLUSIONS

Two different analyses viz, i) varying the number of encoding loops and ii) varying the wavelets are carried out. From the first analysis, it is evident that increasing the number of encoding loops beyond 9 has no significant effect on the obtained results and thus the number of encoding loops is fixed as 9. For the second analysis SPIHT 3D entropy algorithm with nine encoding loops is fixed and the effect of varying the type of wavelets on the compression parameters are analyzed. The impact of varying the wavelets on the compression parameters is very minimal. Regions of interest (ROIs) in medical images, such as the location of lesions or tumors, carry significant information. Thus, a hybrid method of applying lossless compression for ROI and lossy compression on the non ROI regions shows the future directive in the field of medical image compression.

## REFERENCES


[1] A. Martchenko and G. Deng, "Bayesian predictor combination for lossless image compression," in *IEEE Transactions on Image Processing*, vol. 22, no. 12, pp. 5263-5270, Dec. 2013, doi: 10.1109/TIP.2013.2284067.

[2] S. Juliet, E. B. Rajsingh, and K. A. Ezra, “Novel medical image compression using Ripplet transform,” *J Real-Time Image Proc*, vol. 11, pp. 401–412, 2016, doi: 10.1007/s11554-013-0367-9.

[3] H. Jiang, Z. Ma, Y. Hu, B. Yang, and L. Zhang, “Medical image compression based on vector quantization with variable block sizes in wavelet domain,” *Computational intelligence and neuroscience*, 2012, doi: 10.1155/2012/541890.

[4] R. A. DeVore, B. Jawerth, and B. J. Lucier, "Image compression through wavelet transform coding," in *IEEE Transactions on Information Theory*, vol. 38, no. 2, pp. 719-746, Mar. 1992, doi: 10.1109/18.119733.

[5] V. J. Rehna, S. V. Shubhangi, and S. Vasanthi, “Improving the performance of wavelet-based image compression using SPIHT algorithm,” *IRNET transactions on Electrical and Electronics Engineering (ITEEE)*, vol. 1, no. 2, 2012.

[6] A. Islam and W. A. Pearlman, "Embedded and efficient low-complexity hierarchical image coder," in *Proc. SPIE 3653, Visual Communications and Image Processing*, 1998, doi: 10.1117/12.334677.

[7] S. M. Hosseini and A. R. Naghsh-Nilchi, “Medical ultrasound image compression using contextual vector quantization,” *Comput. Biol. Med.*, vol. 42, pp. 743-750, 2012, doi: 10.1016/j.compbiomed.2012.04.006.

[8] J. M. Shapiro, "Embedded image coding using zerotrees of wavelet coefficients," in *IEEE Transactions on Signal Processing*, vol. 41, no. 12, pp. 3445-3462, Dec. 1993, doi: 10.1109/78.258085.

[9] J. Wang and F. Zhang, "Study of the image compression based on SPIHT algorithm," in *2010 International Conference on Intelligent Computing and Cognitive Informatics*, 2010, pp. 130-133, doi: 10.1109/ICICCI.2010.70.

[10] D. Zhao and S. Ma, "Speech compression with best wavelet packet transform and SPIHT algorithm," in *2010 Second International Conference on Computer Modeling and Simulation*, 2010, pp. 360-363, doi: 10.1109/ICCMS.2010.68.

[11] B.-J. Kim and W. A. Pearlman, "An embedded wavelet video coder using three-dimensional set partitioning in hierarchical trees (SPIHT)," in *Proceedings DCC '97. Data Compression Conference*, 1997, pp. 251-260, doi: 10.1109/DCC.1997.582048.
[12] B. J. Kim, Z. Xiong, and W. A. Pearlman, "Low bit-rate scalable video coding with 3-D set partitioning in hierarchical trees (3D-SPIHT)," *IEEE Transaction on Circuits and Systems for Video Technology,* vol. 10, pp. 1374-1387, Dec. 2000.
[13] J. S. Walker, "Wavelet-based image compression," in *transforms and data compression handbook, CPC Press LLC*, 2001.
[14] T. Ramaprabha and M. M. Sathik, "A comparative study of improved region selection process in image compression using SPIHT and WDR," *International Journal of Latest Trends in Computing*, vol. 1, no. 2, 2010.
[15] J. Tian and R. O. Wells, "Embedded image coding using wavelet difference reduction in: Topiwala, P.N. (eds) wavelet image and video compression," *The International Series in Engineering and Computer Science*, vol. 450, 2002, Springer, Boston, MA., doi: 10.1007/0-306-47043-8_17.
[16] B. E. Usevitch, "A tutorial on modern lossy wavelet image compression: foundations of JPEG 2000," *IEEE Signal Processing Magazine*, vol. 18, no. 5, pp. 22-35, Sept. 2001, doi: 10.1109/79.952803.
[17] M. A. Ansari and R. S. Anand, "Context based medical image compression for ultrasound images with contextual set partitioning in hierarchial trees algorithm," *Adv.Eng.Software*, vol. 40, pp. 487-496, 2009, doi: 10.1016/j.advengsoft.2008.08.004.
[18] M. A. Ansari and R. S. Anand, "A novel ROI based algorithm with DCT, wavelet transform and set partitioning in hierarchical trees for medical image compression," *Int. J. Sci. Computing (IJSC),* vol. 2, no. 1, pp. 7-22, 2008.
[19] E. J. Stollnitz, T. D. DeRose, and D. H. Salesin, "Wavelet for computer graphic: theory and applications," *Morgan Kaufman Publisher, USA, San Fransisco*, 1996.
[20] K. R. Namuduri and N. V. Ramaswamy, "Feature preserving image compression," *Pattern Recognition Letters*, vol. 24, no. 15, pp. 2767-2776, Nov. 2003, doi: 10.1016/S0167-8655(03)00120-X.
[21] H. Yang, M. Long, and H. M. Tai, "Region-of-interest image coding based on EBCOT," *IEEE Pro. Image Signal Process.*, vol. 152, no. 5, pp. 590-596, 2013, doi: 10.1049/ip-vis:20041164.
[22] J. C. Garcia-Alvarez, H. Fuhr, and G. Castellanos-Dominguez, "Evaluation of region-of-interest coders using perceptual image quality assessments," *Journal of Visual Commn Image Represent*, vol. 24, no. 8, pp. 1316-1327, 2013, doi: 10.1016/j.jvcir.2013.09.003.
[23] P. E. Sophia and J. Anitha, "Contextual medical image compression using normalized wavelet-transform coefficients and prediction," *IETE Journal of Research*, vol. 63, no. 5, pp. 671-683, 2017, doi: 10.1080/03772063.2017.1309998.
[24] E. Shahhoseini, N. A. Nejad, H. Behnam, and A. Shahhoseini, "A new approach to compression of medical ultrasound images using wavelet transform," in *2010 Third International Conference on Advances in Circuits, Electronics and Micro-electronics*, 2010, pp. 40-44, doi: 10.1109/CENICS.2010.14.
[25] M. D. Manigandan and S. Deepa, "Comprehensive study on the effect of entropy encoding algorithms on medical image compression," *International Research Journal of Engineering and Technology (IRJET),* vol. 5, no. 4, pp. 3460-3468, 2018.


## BIOGRAPHIES OF AUTHORS


**Deepa Sivaraman** is Professor in the Department of Electronics and Communication Engineering in Panimalar Engineering College, Chennai. She received her Bachelor of Engineering degree in electronics and communication engineering from Madras University in the year 1998. She completed her Master's in Engineering in Applied Electronics in the year 2005 and received doctorate in image processing in the year 2014, both from Sathyabama University, Chennai. She has a total teaching experience of about 20 years and her research interest includes wireless communication, image processing, computer vision, pattern recognition, low power VLSI design and architecture. She is a member of ISTE and fellow member of IETE. She can be reached through the email: dineshdeepas1977@gmail.com.



**Jeneetha Jebanazer** currently working as professor in the Department of Electronics and Communication Engineering, Panimalar Engineering College, Chennai. She has a total teaching experience of 18 years. Her research interest includes VLSI design and wireless communication. She received her Bachelor's degree in Electronics and Communication Engineering from Bangalore University in the year 1998. She completed her Master's in the year 2007 in Applied Electronics and Doctorate in VLSI Design in the year 2021 form Dr.MGR Educational and research Institute, Chennai. She can be reached through the email: jeneethaseelan@gmail.com.



**Bhuvaneswari Balasubramanian** is a distinguished scholar in the fields of RF and Microwave and Cognitive Wireless Communication. She is working as Professor in the Department of Electronics and Communication Engineering, Panimalar Engineering College. She completed her BE-ECE in the year 1998 and her ME-Communication Systems in the year 2005. She went on to pursue her Ph.D from Anna University, Chennai and received her Doctorate in the year 2013. She has more than two decades of teaching experience and has spent more than ten years in the field of research. She is a member of ISTE and fellow member of IETE. She has received 1 funded research project from AICTE, New Delhi under RPS, published 8 patents and has over 36 publications to her name. She can be reached through: drbhuvanaramani@gmail.com.